Paste 2023 – GW Wilson, NA Beier, DC Sego, AB Fourie & D Reid (eds)

doi:10.36487/ACG_repo/2355_16

Backfilling in the permafrost: predicting pressure loss and temperature distribution along the paste backfill pipeline system

K Kalonji *Stornoway Diamonds, Canada*

M Mbonimpa *Université du Québec en Abitibi-Témiscamingue, Canada*

T Belem *Université du Québec en Abitibi-Témiscamingue, Canada*

S Ouellet *Agnico Eagle Mines Limited, Canada*

LP Gelinas *Agnico Eagle Mines Limited, Canada*

Abstract

Underground mine backfilling of permafrost open stopes with cemented paste backfill (CPB) has many challenges to overcome, including keeping the CPB unfrozen during pipeline transportation at low pumping costs and ensuring the required strength development under sub-zero temperature conditions. However, CPB strength development depends strongly on the evolution of its internal curing temperature that, in turn, is controlled by the CPB placement temperature (initial) in the stope and by the permafrost boundary temperature. Hence, it is relevant to predict the required pumping pressure and distribution of the CPB temperature along the pipeline by considering the internal and external heat exchanges and the thermo-rheological behaviour of the CPB. The objective of this paper is to simulate the CPB pipe flow in a full-scale pipeline distribution network anticipated for a mine located in the permafrost region of the north of Canada. For that purpose, CPB mixtures were prepared at 10°C (initial temperature expected in the backfill plant) in the laboratory with 5% of type HE Portland cement at a slump height of about 17.8 cm (corresponding to a solid concentration of about 76.3 %). The numerical simulations were performed using the non-isothermal pipe flow model of COMSOL Multiphysics® 5.2 considering a distribution network of approximately 1,600 m long that includes an outdoor section of approximately 294 m exposed to air circulating at a speed of 1 m/s and to an extreme temperature of -50°C. The permafrost temperature was taken to be -5°C. Unheated (at -5°C) and heated (at +2°C) underground openings were studied. A CPB flow velocity of 1.04 m/s and a pipe diameter of 0.1463 m were considered, as proposed by the owner of the mine project. Results indicate that the total pumping pressure is about 12 MPa (heated and unheated stopes) and the pressure gradient ($\Delta p/L$) distribution along the horizontal pipeline sections is about 13 kPa/m. A decrease in the CPB temperature was observed in the surface section, followed by an increase in the underground sections. This temperature increase can be explained by the predominance of heat transfer by convection rather than radial conduction of the heat generated by viscous dissipation. The effect of a thermal insulation of the pipeline section at the surface was also studied for comparison purposes.

Keywords: *cemented paste backfill, permafrost, heat exchange, pumping pressure, pressure gradient, sub-zero temperature, temperature distribution*

1 Introduction

Cemented paste backfill (CPB) is increasingly used in underground mines as a ground support (Brackebusch 1994; Belem & Benzaazoua 2003). Its application in Canada's northern mining operations in permafrost comes with other challenges. One of the major challenges is to keep the CPB unfrozen, even though it is subjected to sub-zero temperatures during transportation in the pipeline distribution network (-50°C at the surface and -5°C underground in the permafrost zone) and during backfill placement in the stope located in

the permafrost zone to ensure the development of the required CPB strength. Exposure to sub-zero temperatures during CPB transport in the pipeline distribution system can lead to its freezing and, consequently, its blockage in that system. Thus the effect of sub-zero temperature on the rheological properties of CPB should be considered when designing the pipeline distribution network to determine the pumping pressure. Kalonji et al. (2015) highlighted the thermal dependence of the CPB rheological properties.

In addition, the strength development of CPB is highly dependent on the evolution of its internal curing temperature. Indeed, the evolution of the CPB internal curing temperature on the mine site strongly depends on the placement temperature of the CPB in underground stopes (Cui & Fall 2016) and also on the heat exchange between the CPB mass and the rock wall (Beya et al. 2019; Mbonimpa et al. 2019). The CPB placement temperature is dependent on the variation of the CPB temperature during its flow in the pipeline distribution network and, consequently, on the heat exchange with the external environment and the internal heat generation due to viscous dissipation and fluid friction. Considering that fresh CPB is a non-Newtonian fluid with high consistency, the heat generation by friction and viscous dissipation is important and should be considered as it plays an important role on the heat transfer (Dehkordi & Memari, 2010). Cooke et al. (1992) highlighted the increase in temperature of the CPB due to viscous dissipation and friction between the CPB and the pipe wall during its transport in the flow loop test system. In addition, in an adiabatic system the increasing temperature of the fluid flowing in a pipeline is proportional to the pressure drop generated by the fluid (Winter 1987). To simulate the curing conditions or the evolution of CPB curing temperature, it is therefore essential to predict the placement temperature of the CPB in the underground stopes.

The objective of this paper is to present a numerical model to determine the pumping pressure of a CPB distribution network, and to predict the evolution of the CPB temperature and the CPB placement temperature considering the thermal dependence of the rheological properties of the CPB, the heat exchange with the external environment, and the heat generated by viscous dissipation and friction between the CPB and the pipe wall.

The pressure gradient ($\Delta p/L$) generated by a flowing fluid in a circular pipe is calculated using the Darcy-Weisbach equation (Swamee & Aggarwal 2011):

$$\frac{\Delta p}{L} = f \frac{\rho\, U^2}{2\ D} \tag{1}$$

where:

U = flow velocity (m/s).

f = Darcy friction factor (–).

D = hydraulic diameter of pipe (m).

L = pipe length (m).

The friction factor f in Equation 1 can be calculated using the following relationship (Assefa & Kaushal 2015):

$$f = \left(f_{lam}^{b} + f_{turb}^{b}\right)^{1/b} \tag{2}$$

The parameter *b* is given by the following relationship:

$$b = 1.7 + \frac{40{,}000}{Re} \tag{3}$$

where:

Re = Reynolds number (–).

The parameters f_{lam} and f_{turb} represent the friction coefficients for laminar and turbulent fluid flow, respectively (Assefa & Kaushal 2015; Swamee & Aggarwal 2011). The parameters f_{lam} and f_{turb} also depend on the type of fluid (Newtonian or non-Newtonian).

A non-Newtonian Bingham fluid is governed by the following relation:

$$\tau = \tau_B + \eta_B \dot{\gamma} \tag{4}$$

where:

τ_o = Bingham yield stress (Pa).

η_B = Bingham plastic viscosity (Pa.s).

Table 1 summarises the formulas used to calculate the parameters f_{lam} et f_{turb} (Farshad et al. 2001; Taylor et al. 2006).

Table 1 Darcy friction factor formulas for Newtonian and non-Newtonian Bingham fluids

Flow regime	Newtonian fluid	Non-Newtonian Bingham fluid
Laminar	$f = \frac{64}{Re}$ with $Re = \frac{\rho D U}{\eta}$	$f_{lam} = \frac{64}{Re} + \frac{10.67 + 0.1414(He/Re)^{1.143}}{[1 + 0.0149(He/Re)^{1.16}]Re}\left(\frac{He}{Re}\right)$ where $Re = \frac{\rho D U}{\eta_B}$ and $He = \frac{\rho D^2 \tau_B}{{\eta_B}^2}$ He = Hedström number (–)
Turbulent	$\frac{1}{\sqrt{f}} = -2\ \log\left[\frac{2.51}{Re\sqrt{f}} + \frac{\varepsilon}{3.71D}\right]$ with $0 \le \varepsilon/D \le 0.05$	$f_{turb} = 4.10^{a_o} \times Re^{-0.193}$ with $a_o = -1.47\left[1 - 0.146\ e^{(-2.9\ 10^{-5} He)}\right]$ Re and He numbers for laminar flow are valid for turbulent flow

Depending on the heat exchange, the increase in fluid temperature during pipeline transport is attributed to heat related to viscous dissipation between fluid layers and internal friction between the fluid and the wall (Winter 1987). The heat related to viscous dissipation depends on the type of fluid (Newtonian or non-Newtonian), the consistency of the fluid, the type of flow and the pipe size (Winter 1987). Thus, the generalised energy equation of a fluid flowing in a cylindrical pipe is given by the following relationship (COMSOL 2012):

$$\rho\ A\ C_p \frac{\partial T}{\partial t} + \rho A C_p U \nabla T = \nabla(A\lambda\nabla T) + \frac{1}{2} f \frac{\rho A}{D} |U|^3 + Q + Q_w \tag{5}$$

where:

A = the cross-sectional area of the pipe.

λ = the thermal conductivity.

C_p (J/kg°C) = the specific or mass heat capacity.

T (°C) = the temperature.

Q (W/m) = the heat source flux (heat related to hydration, for example).

Q_w (W/m) = the heat flux at the wall.

The heat flux at the wall (Q_w) is given by the following relationship (COMSOL 2012):

$$Q_w = h_{loc}(x)\,\pi\,D\,\left(T_w(x) - T_f(x)\right) \tag{6}$$

where:

T_w = wall temperature.

T_f = the fluid temperature.

h_{loc} = the heat transfer coefficient given by the following relationship (Bird et al. 2002; Wagner 2010):

$$h_{loc} = \frac{Nu\,\lambda}{D} \tag{7}$$

where Nu is the Nusselt number. This number reflects the ratio of convective to conductive heat transfer.

For a non-Newtonian fluid (e.g. Bingham) flowing in a cylindrical pipe, the internal Nusselt number Nu can be determined using data providing the variation of Nusselt number Nu with respect to the dimensionless number Ψ for the Herschel Bulkley and Bingham fluids (Cruz et al. 2012; Alves et al. 2015). The dimensionless number ψ is defined by the following relation:

$$\psi = (K/\tau_0)^{1/n}\frac{U}{R} \tag{8}$$

where:

K = fluid consistency index (Pa.s^n).

τ_0 = fluid yield stress (Pa).

n = fluid flow behaviour index (–) and when n = 1, the fluid is a Bingham plastic (viscosity η_B).

R = pipe radius (m).

Similarly, if a forced external convection related to air flow at a given velocity U_{air} and temperature T_{air} around the circular duct is considered, the Nusselt number Nu_{ext} can be calculated using the following expression (Incropera et al. 2007; Ferrouillat et al. 2011):

$$Nu_{ext} = 0.3 + \frac{0.62\sqrt{Re}Pr^{1/3}}{\left[1+(0.4/Pr)^{2/3}\right]^{1/4}}\left[1 + (Re/282\times10^3)^{5/8}\right]^{4/5} \tag{9}$$

where Pr is the Prandtl number and is given by the following relationship:

$$Pr = \frac{C_p\eta}{\lambda} \tag{10}$$

However, Equation 9 is recommended for $Re \times Pr$ >0.2 (Incropera et al. 2007).

2 Experimental program

The experimental program is subdivided into two main stages:

- Physical and mineralogical characterisations of the mine tailings.
- Thermo-rheological and thermal characterisations of CPB.

2.1 Physical and mineralogical characterisations of the mine tailings and backfill mixtures preparation

The Malvern Mastersizer 3000 laser granulometer was used to determine the particle size distribution (PSD) of the tailings. The specific gravity of tailings solids (G_S) grains was measured using the Micromeritics AccuPyc 1330 helium pycnometer. The mineral phases of the tailings were identified by X-ray diffraction (XRD).

Table 2 lists the physical and mineralogical characteristics of the mine tailings X and Y used. In this table, D_x, C_U, C_C and P_y represent, respectively, the diameter corresponding to x% passing on the sieve, the uniformity coefficient, the curvature coefficient and the % passing on the y (µm) sieve. Following the USCS classification system, the mine tailings are low plastic silts (ML). The specific gravity (G_S) of the mine tailings is 2.93. In terms of mineralogy, quartz (40.3%), albite (19.5%), muscovite (14.6%), ankerite (8.8%) and chlorite (8.1%) constitute the major mineral phases of the mine tailings.

The CPB was prepared at a solid mass concentration (C_W) of 76.3%, which corresponds to a standard Abrams cone slump of 17.8 cm using salt water (salt concentration 5 g/L) and type HE Portland cement at a cement-to-tailings ratio (B_w) of 5%. The different ingredients of the CPB (water, cement HE, tailings) were conditioned separately at different temperatures (2, 10 and 20°C) before the CPB mixtures preparation. The CPB was mixed using a laboratory Hobart mixer for 7 minutes.

Table 2 Physical and mineralogical properties of the mine tailings

Parameter	Units	Values
Specific gravity (G_S)	–	2.93
D_{10}	µm	3.1
D_{30}	µm	9.4
D_{50}	µm	18.3
D_{60}	µm	24.4
D_{90}	µm	62.6
$C_C = D_{30}^2/(D_{60}\ D_{10})$	–	1.2
$C_U = (D_{60}/D_{10})$	–	7.7
$P_{2µm}$	%	5.4
$P_{20µm}$	%	53
$P_{80µm}$	%	94
Mineral phases	**Units**	**Values**
Albite	%	19.5
Quartz	%	40.3
Chlorite	%	8.1
Calcite	%	2.4
Actinolite	%	0
Gypsum	%	0
Muscovite	%	14.6
Pyrite	%	0.4
Ankerite	%	8.8
Microline	%	1.3
Magnetite	%	4.6
Total		**100**

2.2 Thermo-rheological and thermal characterisations of CPB

The different ingredients (tailings, water and binder) were conditioned for 24 hours at the targeted testing temperatures before being mixed. The thermo-rheological characterisation of the CPB was performed using the AR 2000 rheometer (TA Instruments) equipped with a vane geometry (diameter 28 mm, height 42 mm) and a cylindrical Peltier system to control the sample temperature during testing with a cylindrical cup (diameter 30 mm). The lateral and bottom gaps were 1 mm and 4 mm, respectively. The continuous ramp flow procedure in steady state flow regime was used. The material was first pre-sheared at a constant shear rate of 100 s^{-1}, then allowed to stand for 15 seconds, and finally subjected to decreasing shear rate steps from 100 to 0 s^{-1} for 70 seconds. The thermo-rheological tests were carried out at 2, 10 and 20°C. The raw rheological test data was processed with Rheology Advantage Data Analysis software. The processing of the raw rheological data was carried out in four steps: stress correction, merging and smoothing, reduction of the number of points or secondary smoothing, and fitting of the rheological model.

Figure 1 presents the rheograms of CPB at 2, 10, and 20°C after the abovementioned raw data processing. The CPB exhibits a non-Newtonian Bingham fluid behaviour. For a given shear rate, the shear stress increases with the increase of the temperature. Figure 2 shows the variation of Bingham shear yield stress and viscosity with temperature. There is an increase in the shear yield stress and Bingham viscosity of CPB with the increase of the temperature between 2 and 20°C. The increase of CPB rheological properties is likely due to the acceleration of binder hydration with increasing temperature (Cooke et al. 1992; Kalonji et al. 2015). This highlights the thermal dependence of the rheological properties of CPB. The established thermal-dependence relationships of Bingham yield stress and viscosity presented in Figure 2 will be incorporated into the COMSOL numerical flow model in the CPB distribution network.

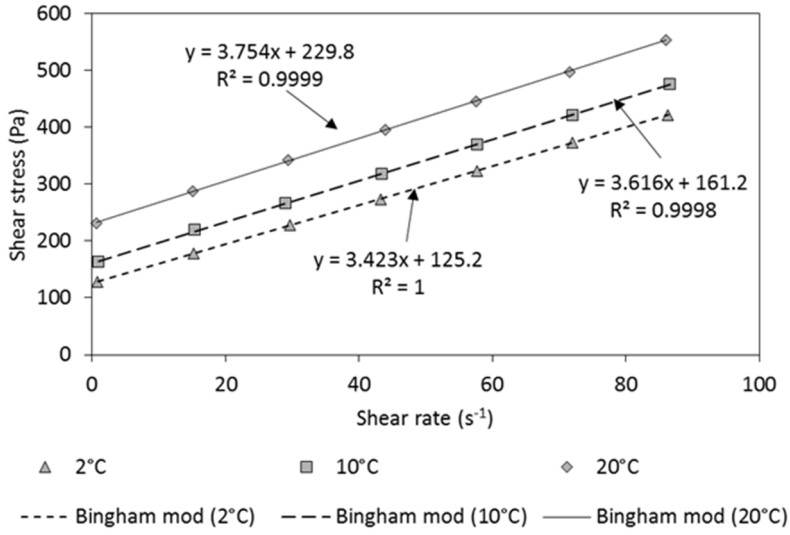

Figure 1 CPB rheograms at 2, 10 and 20°C

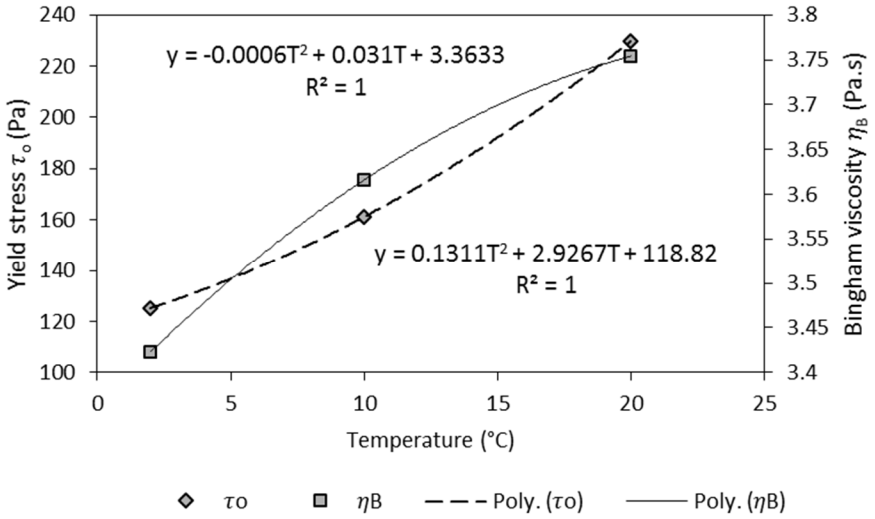

Figure 2 Variation of CPB Bingham yield stress and viscosity as a function of temperature

Thermal properties measurement was performed using the SH-1 probe on the KD2 Pro thermal analyser on a fresh CPB specimen placed in a cylindrical plastic mould (2-inch diameter and 4-inch height). Filling the mould with the CPB sample was performed immediately after mixing with the laboratory Hobart mixer. Subsequently, the SH-1 probe was placed in the fresh CPB sample for the thermal properties' measurement (i.e. thermal conductivity and specific heat capacity).

Figure 3 shows the thermal (temperature range between 2 and 40°C) characterisation results of CPB. It can be observed that the CPB thermal conductivity and specific heat capacity values are almost constant between 2 and 40°C.

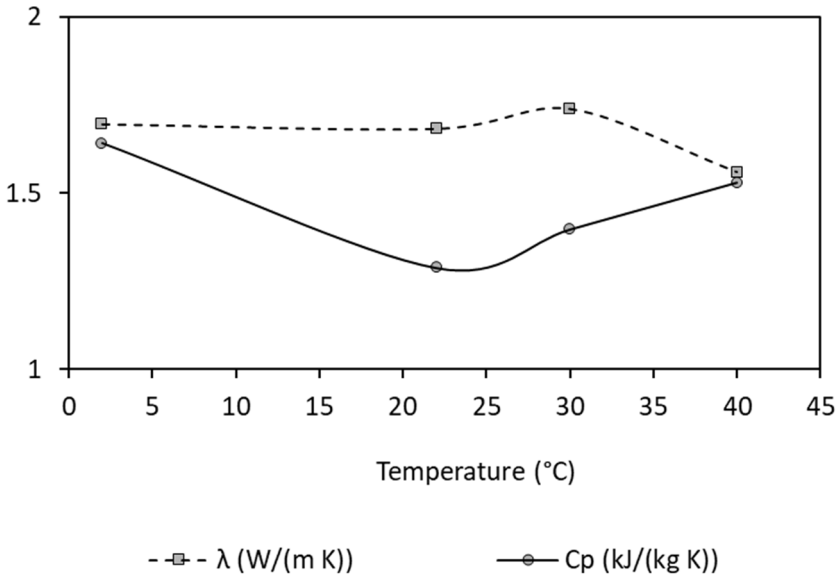

Figure 3 Variation of CPB thermal conductivity and heat capacity as a function of temperature

3 Numerical simulations of CPB flow

The non-isothermal pipe flow numerical model (in 3D stationary mode) of COMSOL Multiphysics® 5.2 was used to simulate the CPB flow and heat transfer in the pipe distribution network. The non-isothermal pipe flow model is a module of the fluid flow interface. It is a coupling of the physical pipe-flow and heat transfer in pipe models, which allows determination of the hydrodynamic (pressure, flow velocity) and heat transfer

(fluid temperature variation, wall heat flux) parameters considering the heat generated by viscous dissipation and internal friction generated by fluid flow in the pipe.

The pipeline distribution network is approximately 1,598.6 m long, consisting of 294.5 m on the surface and 1,304.1 m underground (see Figure 4). The aboveground section is exposed to a wind speed (air) of 1 m/s and a temperature of -50°C. It is assumed that the underground section is also exposed to air flowing at a speed of 1 m/s and temperatures of -5°C (permafrost temperature, not heating the mine) and 2°C (applicable if the mine is heated).

Table 3 summarises the input parameters for the CPB numerical flow model. Due to the marginal variation in thermal properties of CPB between 2 and 20°C, the CPB thermal conductivity and specific capacitance were considered constant (see Table 3).

For the numerical modelling, the external (Nu_{ext}) and internal (Nu) Nusselt numbers must be entered. Equation 9 was used to calculate Nu_{ext} at temperatures ranging from -73 to 27°C and the air velocity of 1 m/s around the 0.1463 m diameter pipe (see Figure 5).

The internal Nusselt (Nu) value listed in Table 3 was determined using Figure 6**Error! Reference source not found.**. For this purpose, the values of the parameter ψ (Equation 8) were first determined based on the variation of rheological properties in the temperature range of 0 and 20°C. It should be noted that the value of Nu considered is the one obtained with the parameter ψ at 10°C (CPB inlet temperature) for the simple reason that Nu varies slightly between 0 and 20°C (i.e. from 4.7 to 5°C).

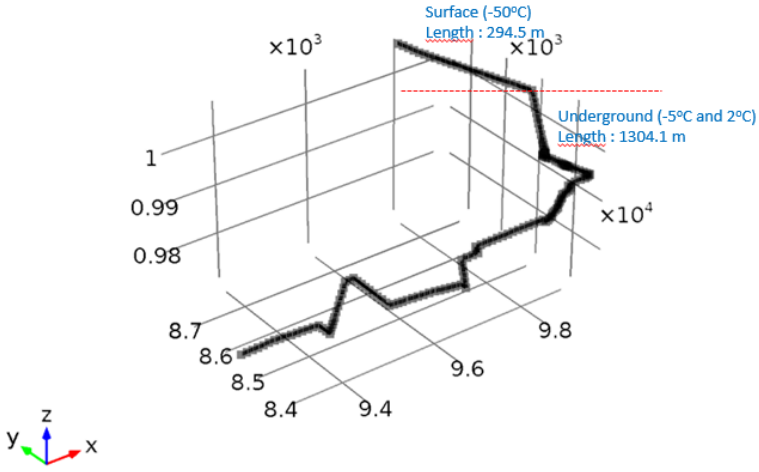

Figure 4 CPB pipeline distribution network

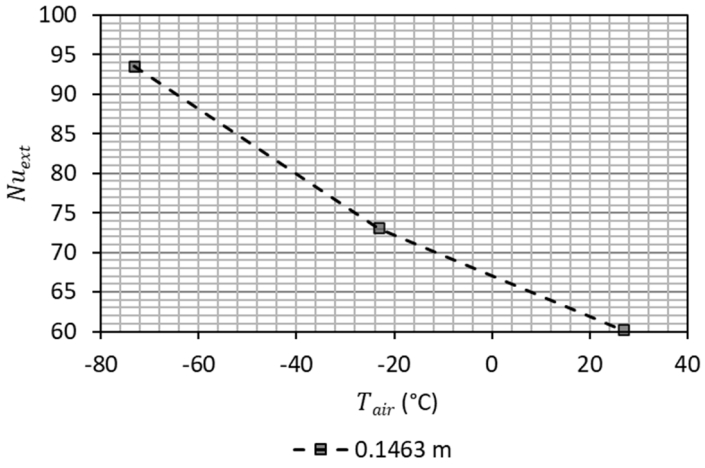

Figure 5 External Nusselt number Nu_{ext} versus external temperature for a pipeline diameter of 0.1463 m and air velocity of 1 m/s

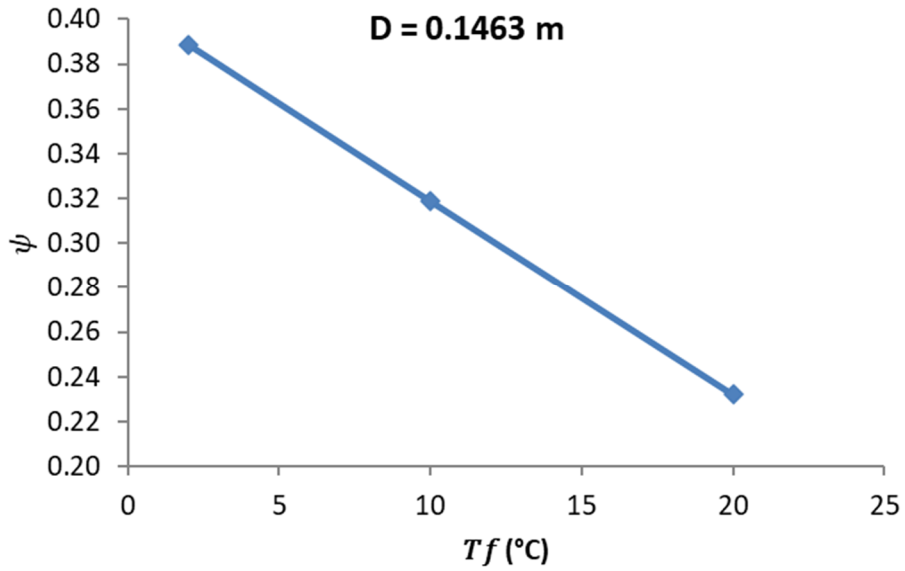

Figure 6 **Dimensionless number ψ versus temperature for D = 0.1463 m, CPB velocity U = 1.04 m/s and CPB rheological properties**

Table 3 **Inlet parameters used for numerical simulations of CPB pressure and temperature in the pipeline distribution network**

Input parameters	CPB
CPB density ρ (kg/m^3)	2,011
CPB solid concentration C_w (%)	76.3
CPB yield stress τ_o (Pa)	See Figure 2
CPB Bingham plastic viscosity η (Pas)	See Figure 2
Thermal conductivity of CPB λ (W/mK)	1.690
Specific heat capacity of CPB C_p (J/kgK)	1,500
Inlet temperature of CPB T_f (°C)	10
Flow velocity of CPB U (m/s)	1.04
Pipe internal diameter D (m)	0.1463
Pipe thermal conductivity (W/mK)	45
Pipe wall thickness (m)	0.025
Surface external temperature T_{air} (°C)	-50
Underground external temperature T_{air} (°C)	2 and -5
Air velocity U_{air} (m/s)	1
Surface external Nusselt Nu_{ext}	84
Underground external Nusselt Nu_{ext}	69 (for -5°C 66 (for 2°C)
Internal Nusselt number Nu	4.9

4 Results and discussion

4.1 Pipe pressure and pressure loss

Figure 7 presents the pressures in the pipeline distribution network and the pressure loss obtained by the CPB flowing at a velocity of 1.04 m/s for the case of heating (at 2°C) and not heating (-5°C) the mine. The pressure values obtained are 11.6 and 11.5 MPa, respectively, for the case of heating (at 2°C) and not heating (-5°C) of the mine. This means that heating the mine does not cause any change in the internal pressures generated in the underground backfill distribution line.

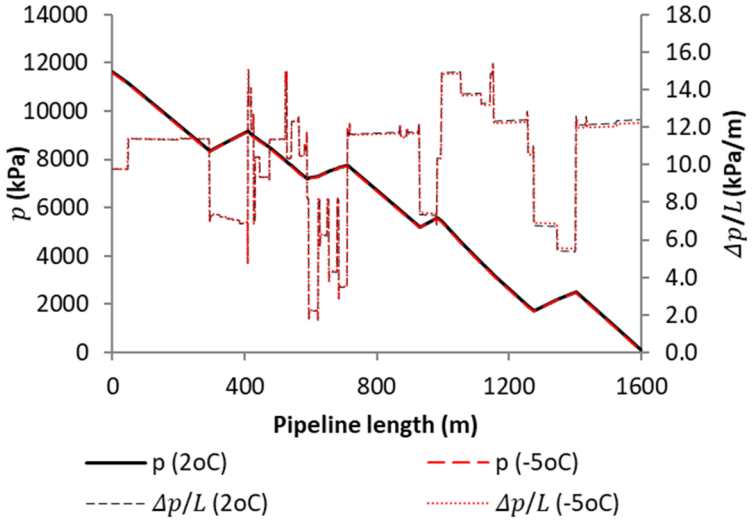

Figure 7 Pressure and pressure loss of CPB flow along the pipeline distribution network

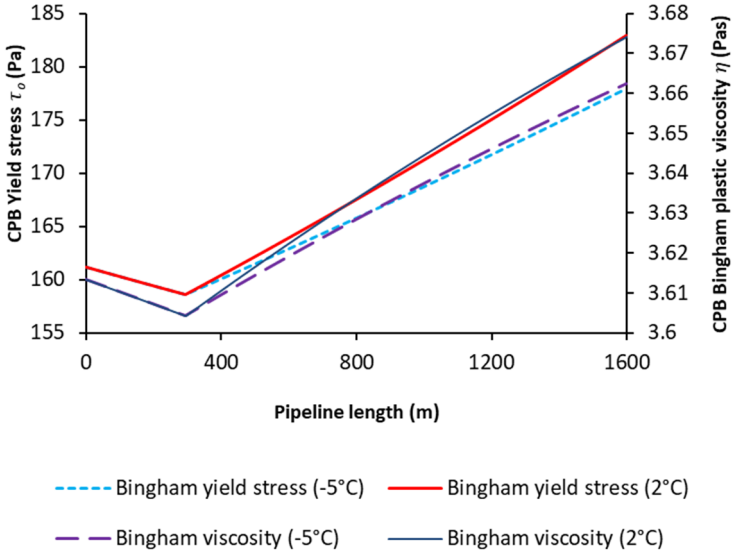

Figure 8 Variation of CPB rheological properties along the pipeline distribution network

The average pressure loss recorded in the horizontal sections are 11.82 kPa/m (6.3 for vertical sections) and 11.76 kPa/m (6.4 for vertical sections), respectively, for the case of heating (to 2°C) and unheating (–5°C) of the mine. It can be noted that the effect of the external underground temperature on the pumping pressures and pressure loss is marginal. This is since in both cases, CPB exhibits almost similar rheological properties during flow through the pipeline distribution system (see Figure 8). The small differences of pressure loss observed over 1,200 m are mainly due to the increase of the CPB temperature difference for both cases (see Figure 9), and consequently on the rheological properties (Figure 8).

4.2 Placement temperature of CPB in the stope

Figure 9 presents the temperature change of CPB flowing at a velocity of 1.04 m/s in the pipeline distribution network. A decrease of CPB temperature in the surface section can be observed up to 9.5°C, then an increase of CPB temperature in the underground section up to 12.8 and 13.6°C, respectively, for underground temperatures of -5 and 2°C. The decrease of CPB temperature in the underground section is related to the very low external temperature (-50°C), which promotes a significant radial conduction heat exchange between the flowing CPB and the pipeline walls.

The thermal insulation was simulated by applying an insulating material (polyurethane) with a thermal conductivity of 0.025 W/mK (Tseng et al. 1997) and a thickness of 0.03 m.

These results indicate that the thermal insulation leads to a decrease in the parietal and radial heat exchange flux, and consequently leads to a low heat loss generated by the viscous dissipation and internal friction of the CPB flow. Thus, there is an increase in the CPB temperature along the entire pipeline. Indeed, the temperature of the CPB increases from 10 to 11°C in the surface section, then increases in the underground sections (with an external temperature of -5°C) up to 14.2°C. The placement temperature of the CPB without thermal insulation was 12.8°C (for an external underground temperature of -5°C).

Table 4 summarises the temperature variation rate during CPB flow in the distribution system. The CPB temperature variation rates during flow in the distribution system are +0.0018, +0.0023 and +0.0027°C/m, respectively, for the uninsulated surface pipe with unheating (-5°C), the uninsulated surface pipe with heating (2°C) of the underground mine, and the insulated surface pipe with unheating (-5°C) of the underground mine.

Table 4 Temperature variation rate of CPB

Cases	CPB temperature variation rate (°C/m)		
	Surface	Underground	Global
Uninsulated surface pipe and heated underground mine (2°C)	–0.0016	+0.0031	+0.0023
Uninsulated surface pipe and unheated underground mine (-5°C)	–0.0016	+0.0025	+0.0018
Insulated surface pipe and unheated underground mine (-5°C)	+0.0032	+0.0025	+0.0027

The option of insulating the pipeline distribution network at the surface is still possible because this study could not show the transverse or radial temperature gradient of the flowing CPB in the pipeline distribution network. Recall that all temperatures shown are those in the pipeline axis.

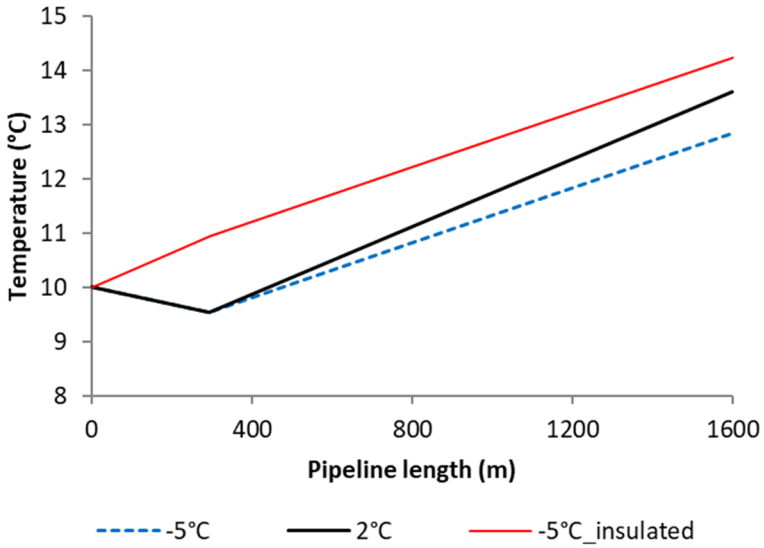

Figure 9 Variation of CPB temperature in the pipeline distribution network for three cases: uninsulated surface pipe with non-heating (-5°C), uninsulated surface pipe with heating (2°C) of the underground mine, and insulated surface pipe with non-heating (-5°C) of the underground mine)

5 Conclusion

The numerical flow model developed in this study determined:

- Pumping pressures of ≈ 12 MPa were required to deliver CPB to the underground stopes.
- Evolution of the CPB temperature as well as the CPB placement temperature in the underground stopes by considering the thermal dependence of the CPB rheological properties.
- Heat exchange with the external environment and the heat generated by the viscous dissipation and friction of the flowing CPB.

This numerical model highlighted that:

- Mine heating had a negligible effect on pumping pressures and head losses. However, heating the mine to 2°C and having an uninsulated surface pipe results in a 0.8°C gain in the CPB placement temperature compared to unheating the mine and having an uninsulated surface pipe.
- A paste backfill placement temperature gain of 1.4°C is observed for the case of unheating the mine and having an insulated surface pipe compared to the case of unheating the mine and having an uninsulated surface pipe.

In the range of variation of the CBP temperature (for the case study) in the pipeline distribution system, there is a small variation in the CPB rheological properties which results in marginal effects on the pumping pressure and the pressure losses.

The numerical model presented has a limitation in that it does not incorporate the effect of pipe wall shear on CPB rheological properties.

Acknowledgment

The authors would like to acknowledge the Fonds de recherche du Québec – Nature et technologies, Agnico Eagle Mines Limited, the Research Institute of Mines and Environment (RIME UQAT-Polytechnique), and the Natural Sciences and Engineering Research Council of Canada for their financial support.

References

Alves, MA, Baptista, A & Coelho PM 2015, 'Simplified method for estimating heat transfer coefficients: constant wall temperature case', *Heat Mass Transfer,* vol. 51, pp. 1041–1047, https://doi.org/10.1007/s00231-015-1509-3

Assefa, KM & Kaushal, DR 2015, 'A comparative study of friction factor correlations for high concentrate slurry flow in smooth pipes', *Journal of Hydrology and Hydromechanics,* vol. 63, pp. 13–20, https://doi.org/10.1515/johh-2015-0008

Belem, T & Benzaazoua, M 2003, 'Utilisation du remblai en pâte comme support de terrain. Partie I : de sa fabrication à sa mise en place sous terre', *Après-mines 2003*.

Beya, FK, Mbonimpa, M, Belem, T, Li, L, Marceau, U, Kalonji, PK, Benzaazoua, M & Ouellet, S 2019, 'Mine backfilling in the permafrost, part I: Numerical prediction of thermal curing conditions within the cemented paste backfill matrix', *Minerals,* vol. 9, pp. 11–20, https://doi.org/10.3390/min9030165

Bird, RB, Stewart, EW & Lightfoot EN 2002, *Transport Phenomena*, 2nd edn, John Wiley and Sons, Inc., New York.

Brackebusch, FW 1994, 'Basics of paste backfill systems', *Mining Engineering*, vol. 46, pp. 1175–1178, https://www.doi.org/10.1016/0148-9062(95)90153-v

COMSOL 2012, *COMSOL Multiphysics Reference Manual*, COMSOL, Burlington, p. 750.

Cooke, R, Spearing, A & Gericke D 1992, 'The influence of binder addition on the hydraulic transport of classified tailings backfills', *Journal of the Southern African Institute of Mining and Metallurgy*, vol. 92, pp. 325–329.

Cruz, DA, Coelho, PM & Alves, MA 2012, 'A simplified method for calculating heat transfer coefficients and friction factors in laminar pipe flow of Non-Newtonian fluids', *ASME Journal of Heat and Mass Transfer*, vol. 134, no. 9, https://doi.org/10.1115/1.4006288

Cui, L & Fall, M 2016, 'Mechanical and thermal properties of cemented tailings materials at early ages: Influence of initial temperature, curing stress and drainage conditions', *Construction and Building Materials*, vol. 125, pp. 553–563, https://doi.org/10.1016/j.conbuildmat.2016.08.080

Dehkordi, AM & Memari, M 2010, 'Transient and steady-state forced convection to power-law fluids in the thermal entrance region of circular ducts: Effects of viscous dissipation, variable viscosity, and axial conduction', *Energy Conversion and Management*, vol. 51, pp. 1065–1074, https://doi.org/10.1016/j.enconman.2009.12.011

Farshad, F, Rieke, H & Garber, J 2001, 'New developments in surface roughness measurements, characterization, and modeling fluid flow in pipe', *Journal of Petroleum Science and Engineering*, vol. 29, no. 2, pp. 139–150, https://doi.org/10.1016/S0920-4105(01)00096-1

Ferrouillat, S, Bontemps, A, Ribeiro, J-P, Gruss, J-A & Soriano, O 2011, 'Hydraulic and heat transfer study of SiO_2/water nanofluids in horizontal tubes with imposed wall temperature boundary conditions', *International Journal of Heat and Fluid Flow*, vol. 32, pp. 424–439.

Incropera, FP, Dewitt, DP, Bergman, TL, & Lavine, AS 2007, *Fundamentals of Heat and Mass transfer*, 6th edn, John Wiley & Son Inc., New York.

Kalonji, K, Mbonimpa, M, Belem, T, Benzaazoua, M, Beya, F & Ouellet, S 2015, 'Preliminary investigation of the effect of temperature and salinity on the rheological properties of fresh cemented paste backfills', *Proceedings of Canadian Geotechnical Conference, GeoQuebec 2015: Challenges from North to South*, Canadian Geotechnical Society.

Mbonimpa, M, Kwizera, P & Belem, T 2019, 'Mine backfilling in the permafrost, part II: Effect of declining curing temperature on the short-term unconfined compressive strength of cemented paste backfills', *Minerals*, vol. 9, no. 3, https://doi.org/10.3390/min9030172

Swamee, PK & Aggarwal, N 2011, 'Explicit equations for laminar flow of Bingham plastic fluids', *Journal of Petroleum Science and Engineering*, vol. 76, pp. 178–184, https://doi.org/10.1016/j.petrol.2011.01.015

Taylor, JB, Carrano, AL & Kandlikar, SG 2006, 'Characterization of the effect of surface roughness and texture on fluid flow—past, present, and future', *International Journal of Thermal Sciences*, vol. 45, pp. 962–968, https://doi.org/10.1016/j.ijthermalsci.2006.01.004

Tseng, C, Yamaguchit, M & Ohmorit, T 1997, 'Thermal conductivity of polyurethane foams from room temperature to 20 K', *Cryogenics*, vol. 37, pp. 305–312.

Wagner, MH 2010, *Heat Transfer to Non-Newtonian Fluids. VDI Heat Atlas 0–5*, Springer, Berlin, https://doi.org/10.1007/978-3-540-77877-6

Winter, HH 1987, 'Viscous dissipation term in energy equations', *American Institute of Chemical Engineers*, vol. 7, pp. 27–34.